Electronic Supplementary Information

Tuning the Acidity and Textural Properties for Enhanced Economical CO_2 Capture in Polyethyleneimine (PEI) Supported Adsorbents

Bitan Ray,[1,2#] Sathyapal R. Churipard,[1,2#] Arjun Cherevotan, Diku Raj Deka,[1,2] Devender Goud,[1,2] Harishankar Kopperi,[1,2] and Sebastian C. Peter[1,2*]

[1]New Chemistry Unit, Jawaharlal Nehru Centre for Advanced Scientific Research, Jakkur, Bangalore-560064
[2]School of Adv. Mater., Jawaharlal Nehru Centre for Advanced Scientific Research, Jakkur, Bangalore-560064
#Authors contributed equally *Corresponding author. Phone: 080-22082998. Email: sebastiancp@gmail.com ; sebastiancp@jncasr.ac.in

Experimental section

Materials: Pseudoboehmite (PSB) (>99%, Sasol), methanol (>99%, Merck), polyethyleneimine (PEI) and (>99%, Sigma Aldrich, M.W. ~800, Mn ~600) were used as obtained without further purification. γ-alumina (γ-Al_2O_3) was prepared by the calcination of pseudoboehmite (PSB) at 550 °C for 4h.

Synthesis

Synthesis of PEI@PSB

The PEI@PSB is prepared by an incipient wetness impregnation method. In a typical synthesis, 0.25 g of polyethyleneimine (PEI) is dispersed in 10 ml methanol under stirring for 10 min in a 100 ml beaker. To the above solution, 1 g of PSB was added and the resulting mixture was stirred at 30 °C for 1h and dried in an oven at 60 °C for 14h. The obtained samples were denoted as 25% PEI@PSB (where 25% indicates the weight % of amine loading). Similarly, different weight percent of PEI was impregnated on different supports such as γ-Al_2O_3 and PSB.

Fourier transform infrared spectroscopy (FTIR) analysis

The successful impregnation of polyethyleneimine (PEI) in the synthesized materials is examined by Fourier transform infrared spectroscopy (FTIR) analysis. The FTIR analysis of powder samples was performed in transmittance mode in the range of 4000-400 cm^{-1}. The analysis was performed by ATR technique and the spectrum was averaged 32 times in every analysis.

Pyridine-IR (Py-IR) analysis

The variation in Brønsted and Lewis acidic sites in unmodified PSB and PEI-impregnated PSB was analyzed by pyridine IR analysis. In a typical experiment, powdered samples were dried at 150 °C in a vacuum for 14 h, cooled and sealed to maintain moisture-free condition. Then the samples were saturated with pyridine under a nitrogen atmosphere and heated at 150 °C for 14 h to remove any

physisorbed pyridine. Then the material was cooled down to room temperature and FTIR analysis was performed in absorbance mode from the wavenumber ranging from 1400 cm^{-1} to 1600 cm^{-1}. Each spectrum of pyridine adsorbed sample was subtracted from that of the pyridine untreated sample to get the peaks specifically due to pyridine interaction with acidic sites in the material.

Static CO_2 uptake experiment

The static CO_2 uptake of the material is determined by CO_2 temperature programmed desorption (TPD) analysis using Altamira AMI-300 Lite instrument. In a typical experiment, around 0.1g of the powder sample was taken in a U-shaped TPD cell. Before the CO_2 adsorption the material was subjected to pretreatment at 150 °C for 1 h with a ramp rate of 10 °C/min under the flow of helium (20ml/min) to remove any adsorbed gases or impurities from the material. Then the material was allowed to cool down to 75 °C and the sample was treated with 10% CO_2 in helium by passing a gas mixture (5 ml/min CO_2 and 45 ml/min helium) for 30 mins. Further, the sample was post-flushed with helium to remove excess physisorbed CO_2. Then the material was again cooled down to 50 °C and the temperature programmed desorption (TPD) analysis was started from 50 °C to 150 °C with a ramp rate of 10 °C with 5 ml/min of helium as carrier gas. The CO_2 desorbed from the sample was detected by using a TCD detector. The amount of CO_2 desorbed from calculated by calibrating the TCD by a known amount of CO_2 after every analysis.

N_2 physisorption experiment

The N_2 physisorption experiment was performed via BELSORP max II physisorption analyzer using N_2 gas as the adsorbate. The experiments were performed at 77 K. The temperature was maintained by keeping liquid Nitrogen in Dewar vessel. The specific surface area and pore size distribution were calculated on the basis of Brunauer–Emmett–Teller (BET) equation and Barret-Joyner-Halenda (BJH) method.

During the experiment small amount of sample (200 – 500 mg) was weighed and transferred into sample tube and vacuumized thoroughly at 75 ℃ for 12 hours to ensure maximum degassing without degrading the amine part present in the samples, prior to the experiment.

Calculation of isosteric heat of adsorption

The CO_2 adsorption experiment was performed via BELSORP max II physisorption analyzer using CO_2 gas as the adsorbate. During the experiment small amount of sample (200 – 500 mg) was weighed and transferred into sample tube and vacuumized thoroughly at 75 ℃ for 12 hours to ensure maximum degassing without degrading the amine part present in the samples, prior to the experiment. The experiments were performed at two different temperatures: 273 K (0 °C) and 298 K (25 °C). The temperature was maintained by keeping methanol in solvent vessel, and a continuous methanol circulation from chiller.

The obtained CO_2 adsorption points were fitted with Freundlich-Langmuir equation (**Eqn. S1**),

$$n = \frac{a \,.\, b \,.\, p^c}{1 + b \,.\, p^c} \qquad \text{Eqn. S1}$$

where n is the amount adsorbed CO_2 in mmol/g, p is the pressure in kPa, a is the maximal loading in mmol/g, b is the affinity constant ($1/kPa^c$) and c is the heterogeneity exponent (the product of $b \cdot p^c$ is a dimension-less parameter. Based on the non-linear curve fitting the a, b, c can be derived and put into the rearranged version of Freundlich-Langmuir equation (**Eqn. S2**).

$$p(n) = \sqrt[c]{\frac{n}{a \,.\, b - n \,.\, b}} \qquad \text{Eqn. S2}$$

A series of p data were derived from the equation, and finally they were replaced accordingly into the Clausius-Clapeyron equation to calculate the isosteric heat of adsorption (**Eqn. S3**).

$$\Delta H_{ads} = -R \,.\, \ln\left(\frac{p_2}{p_1}\right)\frac{T_1 \,.\, T_2}{(T_2 - T_1)} \qquad \text{Eqn. S3}$$

Field-emission Scanning Electron Microscope – Energy Dispersive X-ray (FESEM-EDX analysis

The elemental mapping was performed in Thermofisher Apreo 2S FESEM instrument coupled with EDX. A small amount of the as-synthesized sample was first sonicated with ethanol for 10 minutes and then it was drop-casted over silicon wafer and dried, prior to the analysis.

Powder X-Ray Diffraction (XRD) analysis

The structural stability of the synthesised sorbents was confirmed by powder XRD analysis. The XRD analysis was performed on PANalytical Empyrean X-ray diffractometer with Cu Kα radiation at 45 kV and 40 mA. The measurement was performed using an anti-scatter slit (1°) for an angular range of $10° \leq 2\theta \leq 80°$. The XRD pattern of PEI@PSB and PEI@γ-Al_2O_3 were compared with PSB and γ-Al_2O_3 respectively.

Humid condition CO_2 uptake *via* desorption method

The sample was first exposed to the steam generated by deionised water at 110 ℃ for 2 hours prior to the measurement. Then the humidified material was placed in the U-shapped TPD cell, and it was saturated with CO_2 stream at 75 °C. Followed by the He purging to remove any weakly adsorbed CO_2, the temperature programmed desorption was performed till 150 ℃.

In-situ CO_2 DRIFTS

The in-situ DRIFTS experiment was performed using a Bruker 70v vertex FTIR equipped with a Harrick DRIFTS cell. The spectra were recorded at 4 cm^{-1} resolution and each reading was averaged 32 times. The sample was first activated at 150 ℃ using 1 NLPH nitrogen for 10 mins, and the spectrum of the sample was taken as baseline. Once the temperature is cooled down to 50 ℃, a feed gas containing 1 NLPH CO_2 and 1 NLPH of N_2 is allowed to pass. During this process, at each minute, the spectrum was recorded till the sample is saturated with CO_2.

Life Cycle Assessment (LCA)

The LCA quantifies the various environmental impacts and consequences of products/ processes over their entire lifespan by assessing the possible environment burden.[1, 2] The present study investigated the environmental footprints of the synthesized adsorbent (25% PEI@PSB) having higher capture performance among various studied materials, followed by its potential for CO_2 capture using (LCA) methodology based on ISO 14040/14044 framework.[1-3] The aim is to assess and provide context for produced PEI@PSB at a laboratory scale and extrapolate its carbon capture potential for a standard commercial scale approach.[4] Initially, the work focus on analysis of synthesised 25% PEI@PSB followed by its utilization of catalyst for carbon capture (CC), with 1 ton CC as the functional unit (FU). This work considered an ex-ante 'cradle-to-grave' scope approach that incorporates the complete product capture. The spatial scope depends on the synthesis of 25% PEI@PSB, while temporal scope is set to conduct a carbon capture potential to assess the environmental effects of 25% PEI@PSB for CC scale up. The second phase involves, designing a system boundary (from synthesis to final capture) and life cycle inventory (LCI). **Figure S19** illustrates the inputs (with two ratios; Case-A and Case B) and output flows for 25% PEI@PSB and CC system. The LCI comprises chemicals inputs, energy input, natural resources, and by-products for catalyst and CC (**Table S6**). The proxy LCI data (Step-1: 25% PEI@PSB synthesis) for chemicals, such as Pseudoboehmite, were obtained by substituting aluminium metal oxides instead of entirely eliminating the inputs to LCIs. A linear scaling up of the input material balance were performed using the lab scale experimental yields from 100 cycles for CC that were investigated. The energy inputs were determined by considering the process flows and specific heat of the material.[5, 6] The LCI scenarios were assessed using SimaPro (v 9.6.0.1) software, and ecoinvent database (v 3.10) for background processes with 'cut-off' approach. The study utilized two life cycle impact assessment (LCIA) approaches, namely the ReCiPe 2016 end-point (H) having three sub categories and midpoint (H) (v 1.08) with 18 sub categories.[7, 8] Moreover, environmental impact deviations of energy, we examined two primary electricity sources: Non-renewable (NRE: Coal-Indian-Southern grid) and Renewable energy (RE: Solar-photovoltaic). The energy alternatives examined in this study offer a comparative analysis of the current grid and renewable alternatives, particularly in relation to emissions and energy consumption scale, which is an increasing issue.[2, 9] The CO_2 inputs

were obtained from the LCI database. Various methods for supplying CO_2, includes CO_2 capture from flue gas (namely CO_2 from fossil-fired power plants or industrial processes).[9-11]

Schemes

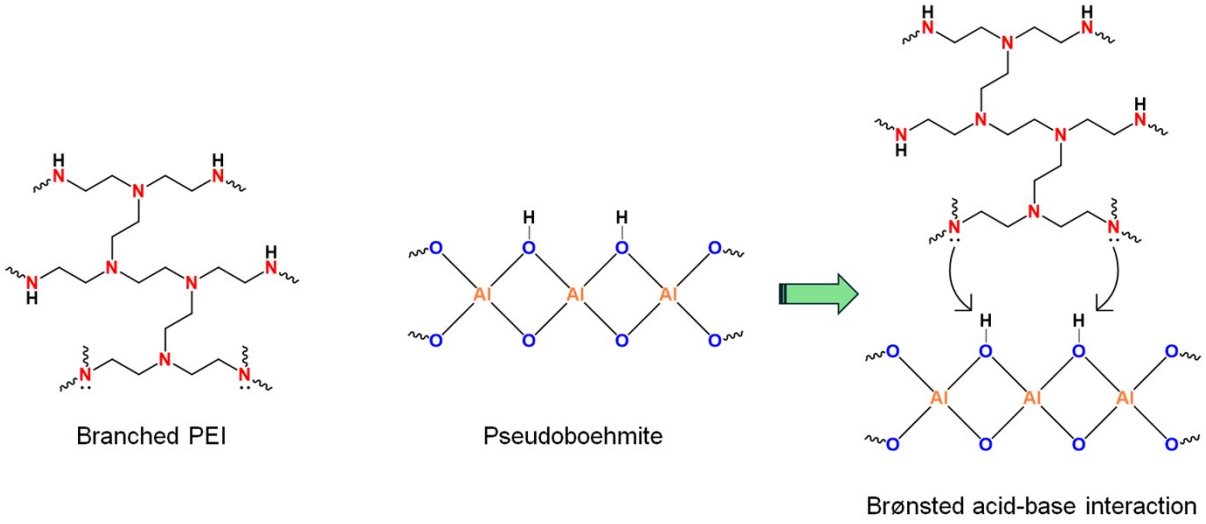

Scheme S1. Synthesis of PEI-PSB depicting the predominant Brønsted acid-base interaction between PEI and Brønsted acid sites in PSB

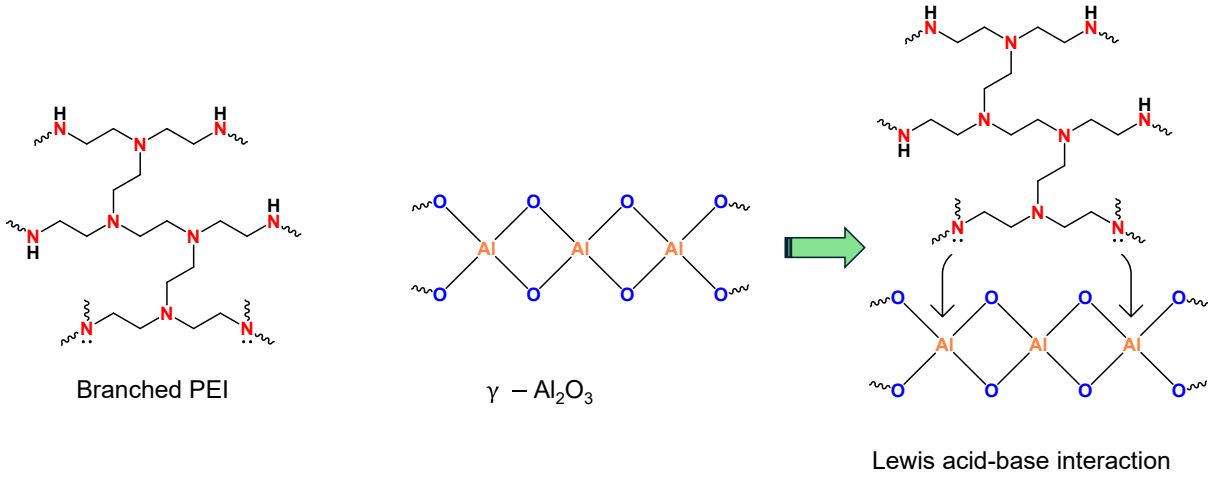

Scheme S2. Synthesis of PEI-Al_2O_3 depicting the predominant Lewis acid-base interaction between PEI and Lewis acid sites in γ−Al_2O_3.

Tables

Table S1. Comparison of CO_2 adsorption performance of PEI-based sorbents

Material	Adsorption Temp. (°C)	Desorption Temp. (°C)	CO_2 uptake (mmol/g)
10% PEI@PSB	75° C	150°C	1.6
20% PEI@PSB	75° C	150°C	3.4
25% PEI@PSB	**75° C**	**150°C**	**4.9**
30% PEI@PSB	75° C	150°C	4.7
40% PEI@PSB	75° C	150°C	3.7
20% PEI@γ-Al_2O_3	75° C	150°C	2.3
25% PEI@γ-Al_2O_3	75° C	150°C	3.2
30% PEI@γ-Al_2O_3	75° C	150°C	3.0
25% PEI@ZSM-5	75° C	150°C	4.7
25% PEI@SBA-15	75° C	150°C	1.6

Table S2: Literature summary of some of the best PEI-based adsorbents for CO_2 capture

Support	Amine type	Amine loading (%)	Adsorption Temp. (°C)	Regeneration Temp. (°C)	Type	CO_2 [a] uptake (mg/g)	CO_2 [b] uptake (mg/g)	CO_2 uptake (mmol/g)	Ref.
PSB	**PEI**	**25**	**75**	**200**	**Static**	**225**	**151**	**5.1**	**Our work**
PSB	**PEI**	**25**	**75**	**150**	**Static**	**216**	**211**	**4.9**	**Our work**
MCM-41	PEI	50	75	75	Static	108	103	2.5	[12]
MCM-41	PEI	75	75	-	Static	133	101	3.0	[13]
MCM-41	PEI	75	75	-	Static	246	-	5.6	[14]
MCM-41	PEI	55	75	-	Static	-	-	4.7	[15]
Si-MCM-41	PEI	75	75	-	Static	133	101	3.0	[16]
SBA-15	PEI	50	75	110	Static	174	166	4.0	[17]
Silica gel	PEI	30	40	130	Static	207	121	4.7	[18]
Resin	PEI	30	65	110	Static	176	158	4.0	[19]
Silica foam	PEI	80	75	-		-	-	5.8	[20]
Al_2O_3	PEI	40	90	120	Static	116	110	2.6	[21]
Al_2O_3	PEI	50	90	120	Static	125	124	2.8	[21]
Al_2O_3	PEI	20	75	75	Static	70	63	1.6	[22]
Al_2O_3	PEI	55	90	165	Static	134	112	3.0	[23]
Al_2O_3	PEI	55	90	165	Static	132	93	3.0	[23]
Al_2O_3	PEI	45	75	75	Static	119	116	2.7	[24]
Al_2O_3	PEI	25	75	100	Static	50	44	1.1	[25]
γ-Al_2O_3	PEI	25	75	100	Static	43	35	1.0	[26]
Al_2O_3	PEI	19	35	100	Static	56	53	1.3	[27]
Al_2O_3	PEI	30	75	75	Static	74	68	1.7	[28]
SiO_2	PEI	50	90	150	Static	101	13	2.3	[29]
SiO_2	PEI	40	90	150	Static	134	25	3.0	[30]
SiO_2	PEI	60	105	150	Static	116	38	2.6	[31]
SiO_2	PEI	50	40	120	Static	128	48	2.9	[32]
SiO_2	PEI	40	90	120	Static	125	124	2.8	[21]

[a] initial CO_2 uptake of adsorbent

[b] final CO_2 uptake after regeneration cycles

Table S3. Summary of N_2 physisorption measurements.

Materials	BET Surface Area (m^2g^{-1})[a]	BJH Pore Distribution (nm)[b]	Pore Volume (cm^3g^{-1})
PSB	228.2	6.9	0.3618
20% PEI@PSB	81.9	6.1	0.1839
25% PEI@PSB	49.8	6.8	0.1253
30% PEI@PSB	24.4	8.4	0.0788
40% PEI@PSB	N/A	N/A	N/A
γ-Al_2O_3	193.9	9.2	0.4613
25% PEI@γ-Al_2O_3	70.3	7.9	0.1982
ZSM-5	389.8	1.7	0.2814
SBA-15	851.2	7.3	0.8773

a = From BET

b = Pore size distribution by BJH method

c = Pore size distribution by MP-plot method

Table S4. Relative concentration of BAS and LAS and B/L ratio

Entry	Material	BAS	BAS and LAS	LAS	B/L
1	PSB	3	2.3	4.9	0.61
2	Gamma alumina	1.2	0.9	2.2	0.56
3	15% PEI@PSB	0.9	0.7	1.6	0.56
4	20% PEI@PSB	1.6	1.2	2.9	0.56
5	**25% PEI@PSB**	**3.6**	**2.9**	**6.2**	**0.58**
6	30% PEI@PSB	2.0	1.6	3.8	0.53
7	25% PEI@ γ-Al_2O_3	3.0	6.2	12.0	0.25
8	ZSM-5	3.3	4.4	7.4	0.45
9	SBA-15	7.9	10.5	N/A	N/A

Table S5. Effect of desorption temperature on 25% PEI@PSB

Material	Adsorption temperature (°C)	Desorption temperature (°C)	CO_2 uptake (mmol/g)
25PEI@PSB	75	150	4.9
25PEI@PSB	75	175	4.9
25PEI@PSB	75	200	5.1

Table S6. Inventory for the adsorbent synthesis and carbon capture for the studies 25% PEI@PSB for Case-A and Case-B.

Case-A	Requirements	Inputs	Product yield (grams)	Byproducts
Step 1 Adsorbent preparation	Reagent	Branched Polyethyleimine 1157.5 kg	25% PEI@PSB 4630 kg	–
	Starting Material	Pseudoboehmite 4630 kg		–
	Solvents	Methanol: 92 L		recoverable
	Stirring	Stirring: 1 hr (2.4 kW × 1 h = 2.4 kWh)		–
	Temperature (mode of heating)	60 ℃ for 14 hrs (0.5 kW × 14 h = 7 kWh)		–
Step 2 CO_2 capture studies **Desorption Temp. 150 ℃**	Starting Material	25% PEI@PSB: 4630 kg Feed: 10 % CO_2/He	1 ton CO_2 capture Required adsorbent = 4629.63 (4630) kg	–
	Duration (TPD Run)	210 mins (4.4 kW × 3.5 h = 15.4 kWh)		–
Case-B	**Requirements**	**Inputs**	**Product yield (grams)**	**Byproducts**
Step 1 Adsorbent preparation	Reagent	Branched Polyethyleimine 1111 kg	25% PEI@PSB 4444 kg	–
	Starting Material	Pseudoboehmite 4444 g		–
	Solvents	Methanol: 88 L		recoverable
	Stirring	Stirring: 1 hr (2.4 kW × 1 h = 2.4 kWh)		–
	Temperature (mode of heating)	60 ℃ for 14 hrs (0.5 kW × 14 h = 7 kWh)		–
Step 2 CO_2 capture Studies **Desorption Temp. 200 ℃**	Starting Material	25% PEI@PSB: 4444 mg Feed: 10 % CO_2/He	1 ton CO_2 capture Required adsorbent = 4444.44 (4444) kg	–
	Duration (TPD Run)	240 mins (4.4 kW × 4 h = 17.6 kWh)		–

Table S7. Damage categories for the 25% PEI@PSB in Case-A and Case-B.

Damage category	Unit	Case A	Case B
Human health	DALY	0.015398849	0.015400125
Ecosystems	species.yr	1.77E-05	1.77E-05
Resources	USD2013	293.5	293.75

Table S8. Impact categories for the Carbon capture with 25% PEI@PSB in Case-A and Case-B

Impact category	Unit	Case-A	Case-B
Global warming	kg CO_2 eq	3700.90	3701.6
Stratospheric ozone depletion	kg CFC11 eq	0.0007	0.0007
Ionizing radiation	kBq Co-60 eq	87.19	87.20
Ozone formation, Human health	kg NO_x eq	10.77	10.7
Fine particulate matter formation	kg PM2.5 eq	6.90	6.90
Ozone formation, Terrestrial ecosystems	kg NO_x eq	11.03	11.03
Terrestrial acidification	kg SO_2 eq	19.001	19.00
Freshwater eutrophication	kg P eq	1.5	1.50
Marine eutrophication	kg N eq	2.06	2.06
Terrestrial ecotoxicity	kg 1,4-DCB	7422.1	7422.9
Freshwater ecotoxicity	kg 1,4-DCB	197.63	197.6
Marine ecotoxicity	kg 1,4-DCB	274.68	274.7
Human carcinogenic toxicity	kg 1,4-DCB	1894.6	1894.6
Human non-carcinogenic toxicity	kg 1,4-DCB	5623.7	5624.09
Land use	m^2a crop eq	42.89	42.9
Mineral resource scarcity	kg Cu eq	124.7	124.76
Fossil resource scarcity	kg oil eq	994.8	995.5
Water consumption	m^3	25.94	25.94

Table S9. Damage categories for the carbon capture with 25% PEI@PSB in Case-A and Case-B: renewable energy (RE) and non-renewable energy (NRE) grid.

Damage category	Unit	NRE		RE	
		Case-A	Case-B	Case-A	Case-B
Human health	DALY	5.90E-05	6.72E-05	3.31E-06	3.56E-06
Ecosystems	species.yr	8.97E-08	1.02E-07	5.52E-09	6.05E-09
Resources	USD2013	0.41	0.46	0.103	0.11

Table S10. LCA of impact categories for the carbon capture with 25% PEI@PSB in Case-A and Case-B: renewable energy (RE) and non-renewable energy (NRE) grid.

Impact category	Unit	NRE		RE	
		Case A	Case B	Case-A	Case-B
Global warming	kg CO_2 eq	19.08	21.75	1.09	1.19
Stratospheric ozone depletion	kg CFC11 eq	4.87E-06	5.55E-06	1.68E-07	1.82E-07
Ionizing radiation	kBq Co-60 eq	0.88	1.01	0.017	0.01
Ozone formation, Human health	kg NO_x eq	0.042	0.04	0.0022	0.0025255
Fine particulate matter formation	kg PM2.5 eq	0.04	0.05	0.0014	0.0015
Ozone formation, Terrestrial ecosystems	kg NO_x eq	0.04	0.04	0.0023	0.0025
Terrestrial acidification	kg SO_2 eq	0.06	0.07	0.0037	0.0040
Freshwater eutrophication	kg P eq	0.01	0.02	0.00027	0.0002
Marine eutrophication	kg N eq	0.001	0.001	0.00021	0.0002
Terrestrial ecotoxicity	kg 1,4-DCB	44.11	50.31	3.79	4.23
Freshwater ecotoxicity	kg 1,4-DCB	1.1	1.28	0.06	0.07
Marine ecotoxicity	kg 1,4-DCB	1.4	1.68	0.09	0.10
Human carcinogenic toxicity	kg 1,4-DCB	1.4	1.59	0.34	0.36
Human non-carcinogenic toxicity	kg 1,4-DCB	28.5	32.5	0.98	1.04
Land use	m^2a crop eq	0.28	0.32	0.11	0.12
Mineral resource scarcity	kg Cu eq	0.03	0.03	0.024	0.02
Fossil resource scarcity	kg oil eq	4.75	5.42	0.319	0.35
Water consumption	m^3	0.10	0.12	0.006	0.007

Table S11. Summary of CO_2 uptake experiments in dynamic mode

Materials	Breakthrough Time (seconds)	Uptake till Breakthrough Point q_b
20% PEI@γ-Al_2O_3	19.5	1.63 ml of $CO_2/g_{sorbent}$ 3.19 mg of $CO_2/g_{sorbent}$
25% PEI@γ-Al_2O_3	33.5	2.79 ml of $CO_2/g_{sorbent}$ 5.47 mg of $CO_2/g_{sorbent}$
30% PEI@γ-Al_2O_3	23.5	1.96 ml of $CO_2/g_{sorbent}$ 3.84 mg of $CO_2/g_{sorbent}$
20% PEI@PSB	25.0	2.08 ml of $CO_2/g_{sorbent}$ 4.08 mg of $CO_2/g_{sorbent}$
25% PEI@PSB	34.5	2.88 ml of $CO_2/g_{sorbent}$ 5.64 mg of $CO_2/g_{sorbent}$
30% PEI@PSB	26.0	2.17 ml of $CO_2/g_{sorbent}$ 4.25 mg of $CO_2/g_{sorbent}$

Table S12. Comparison of CO_2 adsorption performance at humid conditions

Material	Adsorption Temp. (°C)	Desorption Temp. (°C)	CO_2 uptake (μmol/g)
γ-Al_2O_3	75° C	150°C	873.13
25% PEI@ γ-Al_2O_3	75° C	150°C	5343.3
PSB	75° C	150°C	919.81
25% PEI@PSB	75° C	150°C	3916.7

Figures

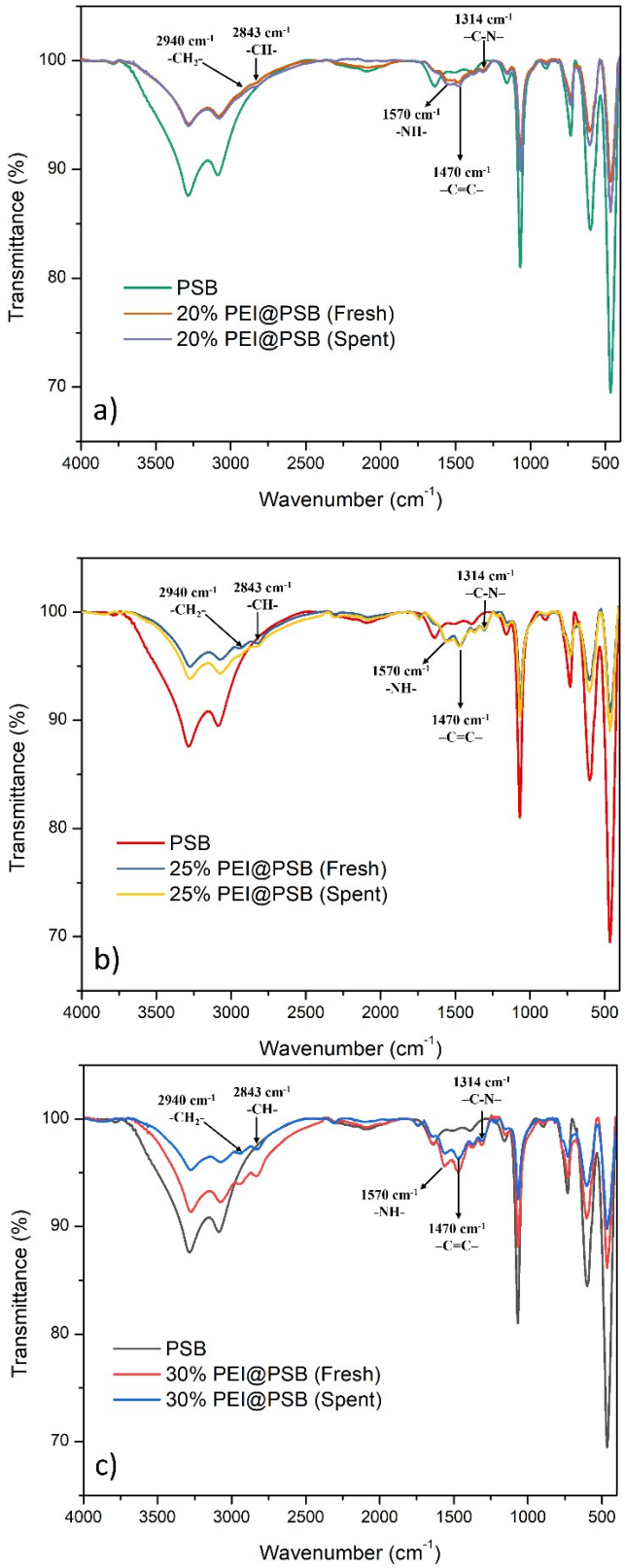

Figure S1. FTIR spectra of a) unmodified PSB, fresh 20% PEI@PSB and spent 20% PEI@PSB, b) unmodified PSB, fresh 25% PEI@PSB and spent 25% PEI@PSB, c) unmodified PSB, fresh 30% PEI@PSB and spent 30% PEI@PSB.

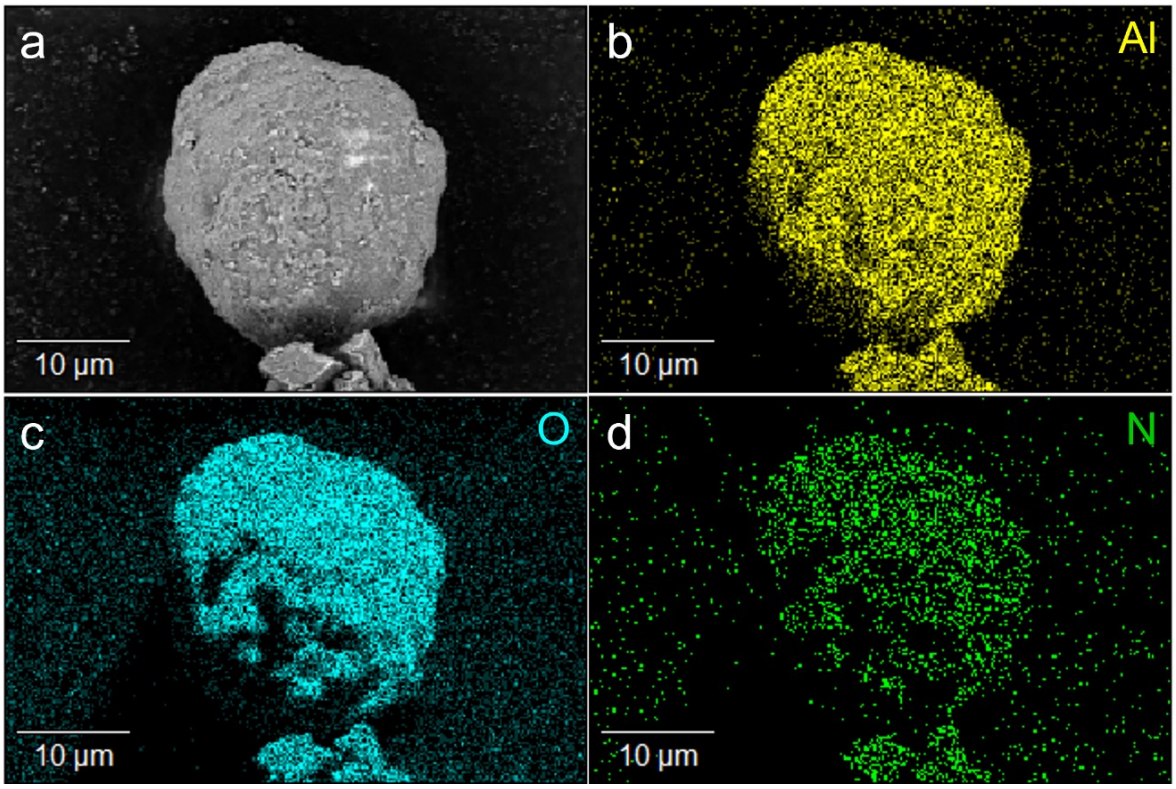

Figure S2. SEM image of (a) 20% PEI@PSB and elemental mapping, (b) nitrogen, (c) carbon, and (d) oxygen.

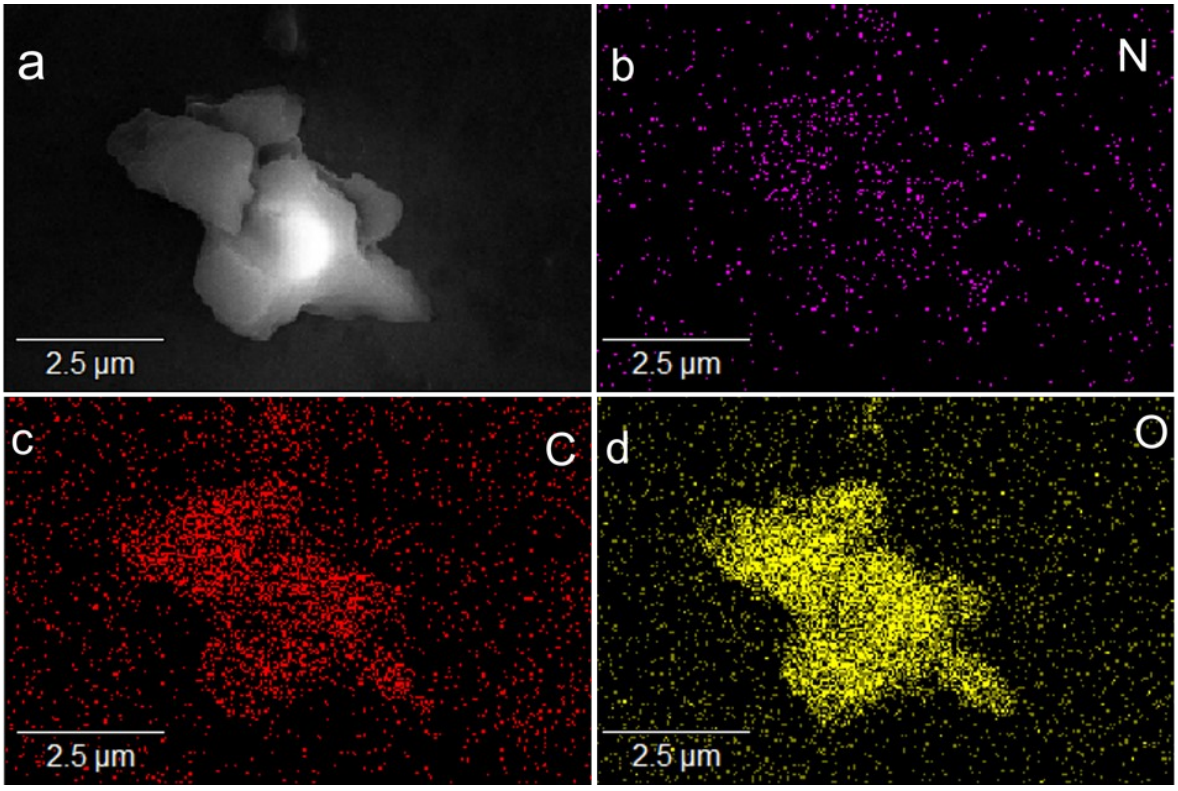

Figure S3. SEM image of (a) 25% PEI@PSB and elemental mapping, (b) nitrogen, (c) carbon, and (d) oxygen.

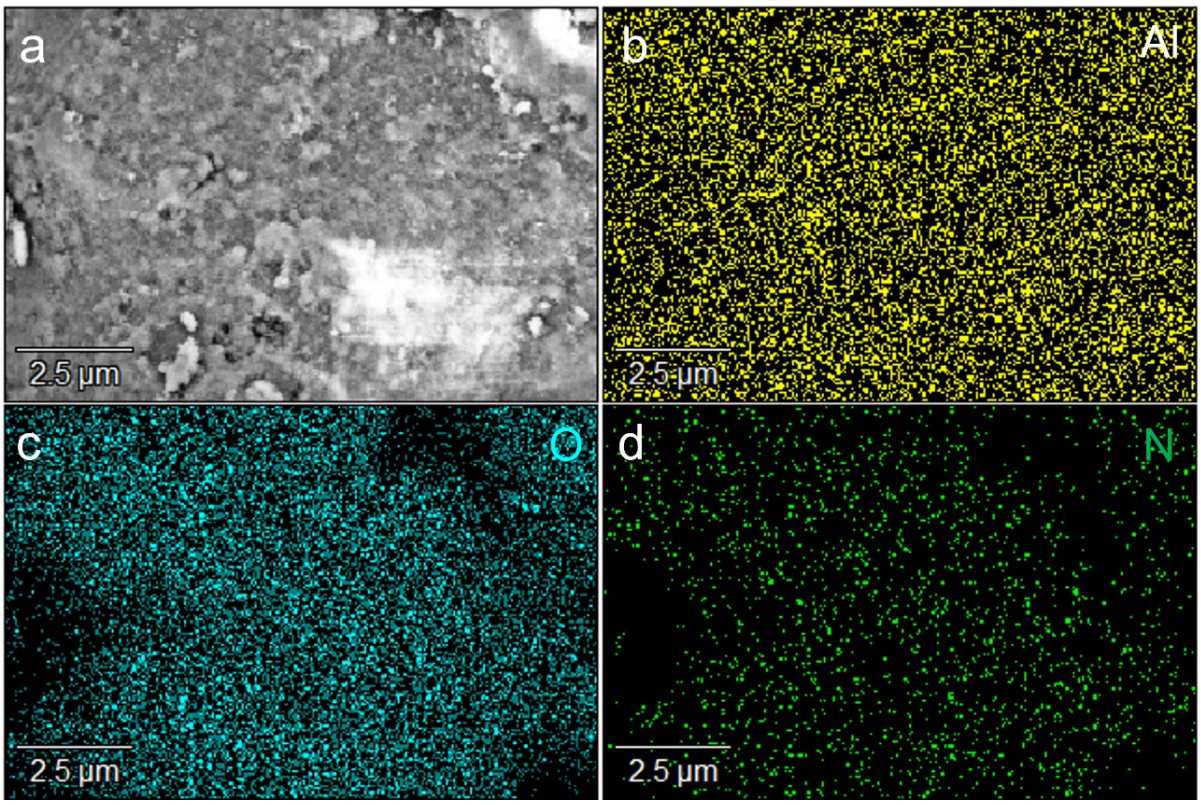

Figure S4. SEM image of (a) 30% PEI@PSB and elemental mapping, (b) nitrogen, (c) carbon, and (d) oxygen.

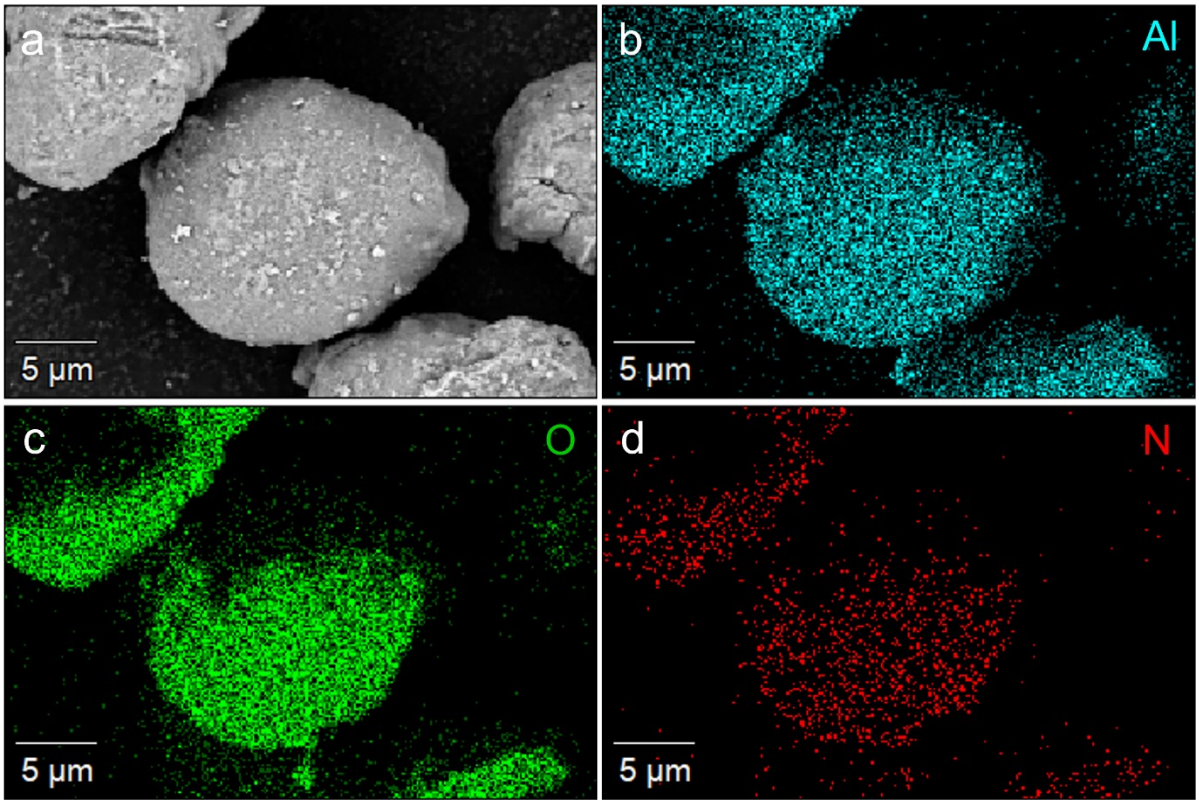

Figure S5. SEM image of (a) 20% PEI@γ-Al_2O_3 and elemental mapping, (b) nitrogen, (c) carbon, and (d) oxygen.

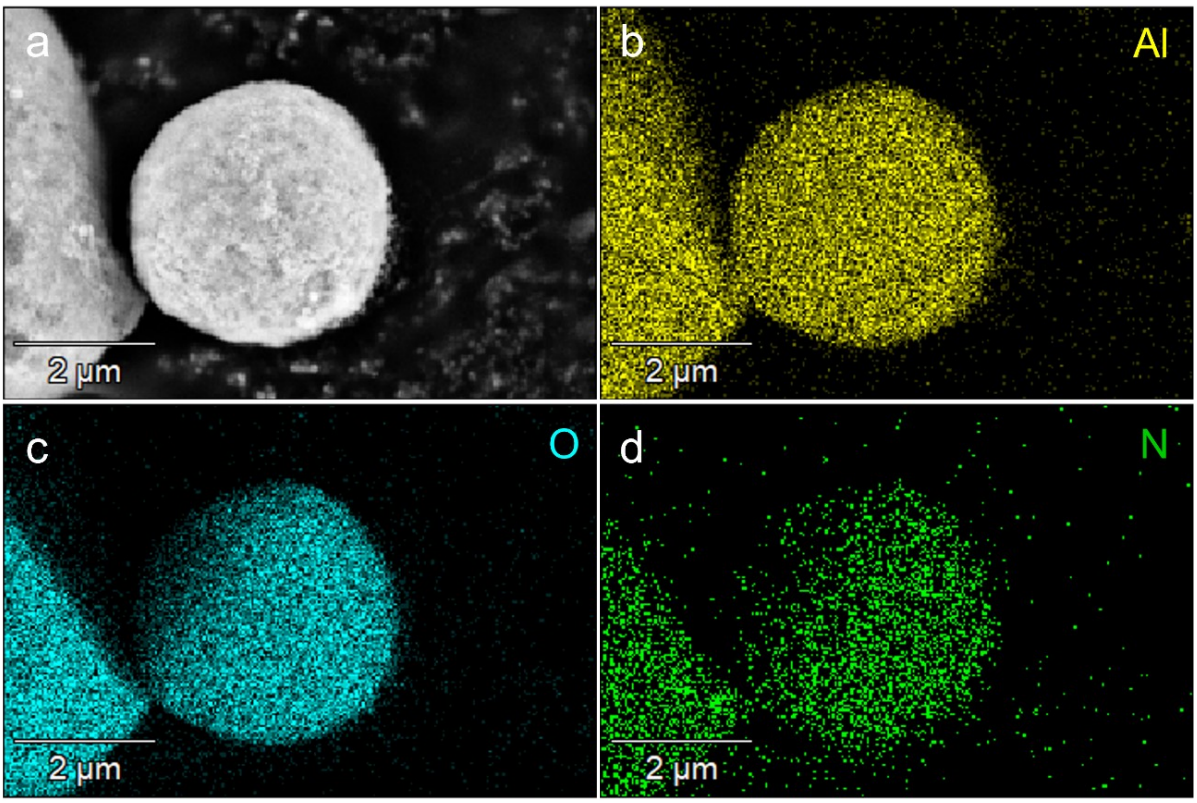

Figure S6. SEM image of (a) 25% PEI@γ-Al_2O_3 and elemental mapping, (b) nitrogen, (c) carbon, and (d) oxygen.

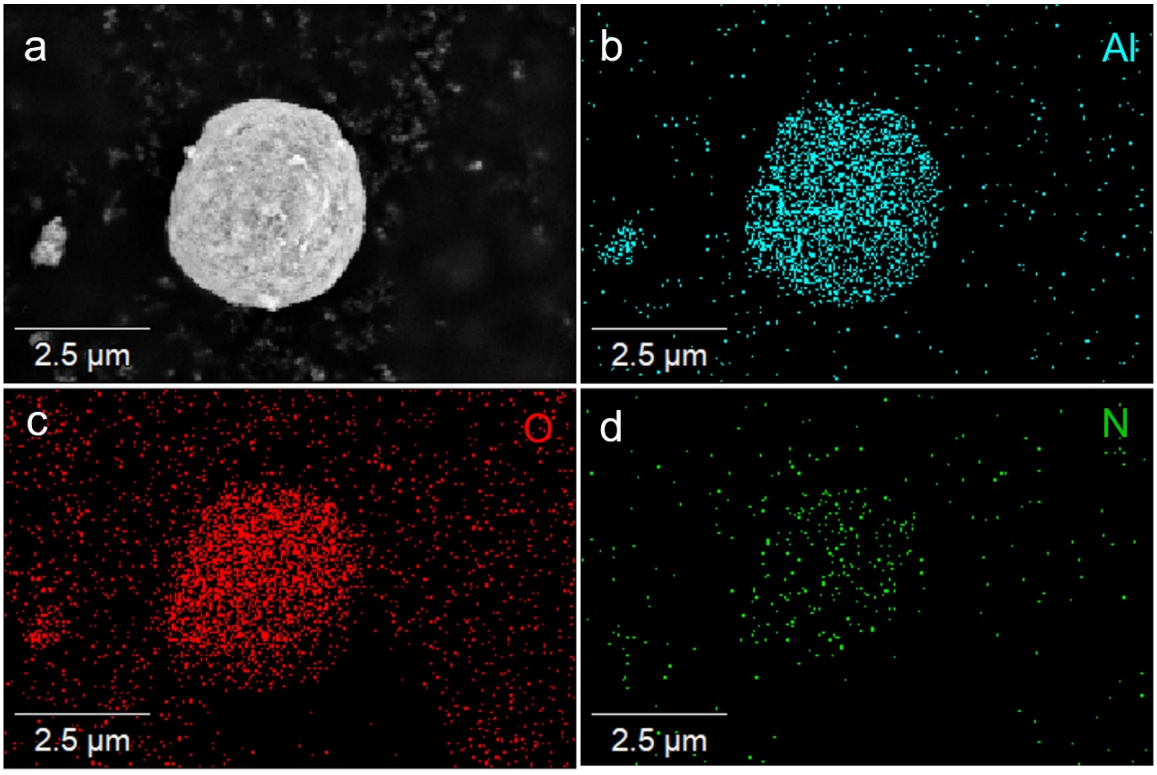

Figure S7. SEM image of (a) 30% PEI@γ-Al_2O_3 and elemental mapping, (b) nitrogen, (c) carbon, and (d) oxygen.

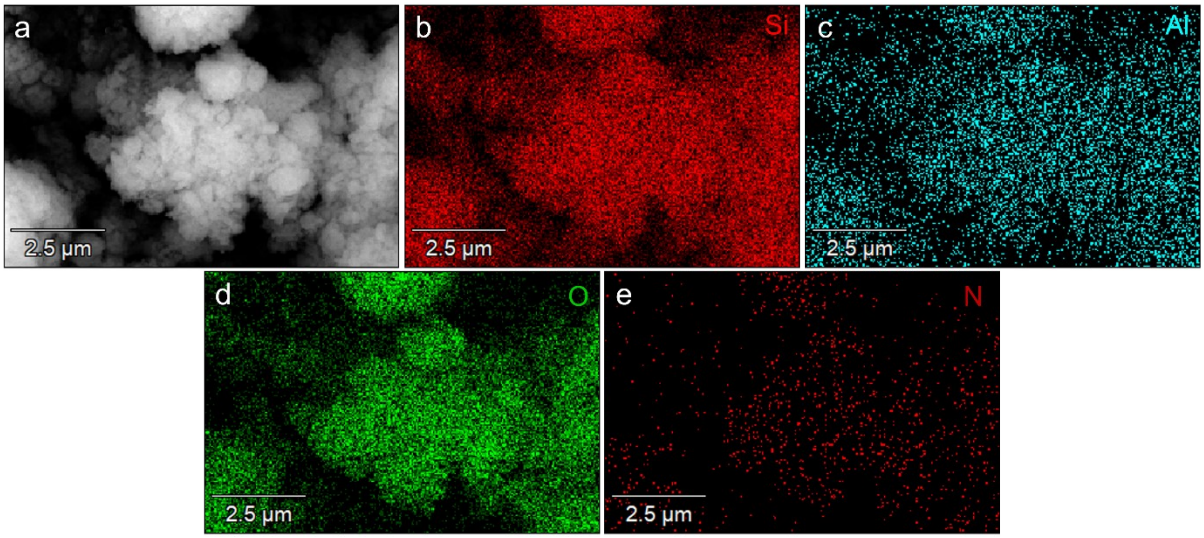

Figure S8. SEM image of (a) 25% PEI@ZSM-5 and elemental mapping, (b) nitrogen, (c) carbon, and (d) oxygen.

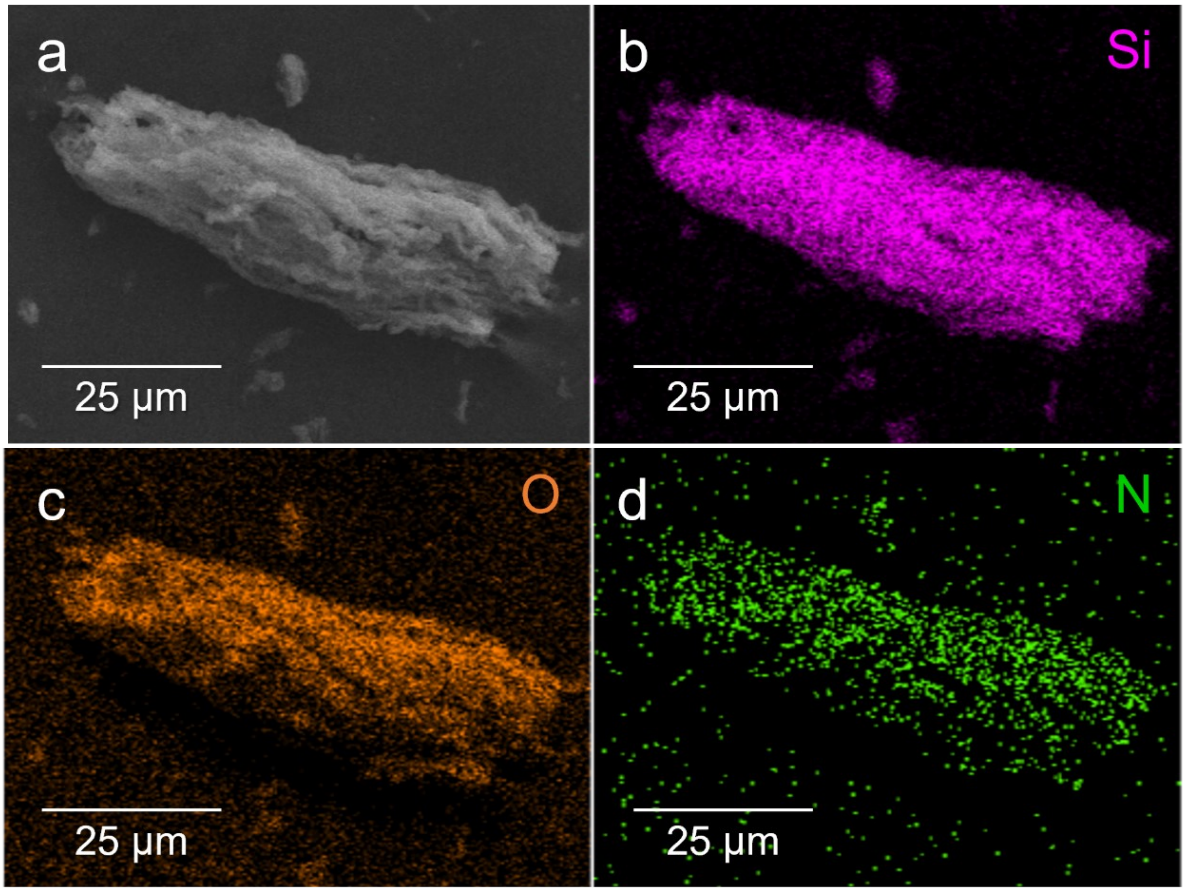

Figure S9. SEM image of (a) 25% PEI@SBA-15 and elemental mapping, (b) nitrogen, (c) carbon, and (d) oxygen.

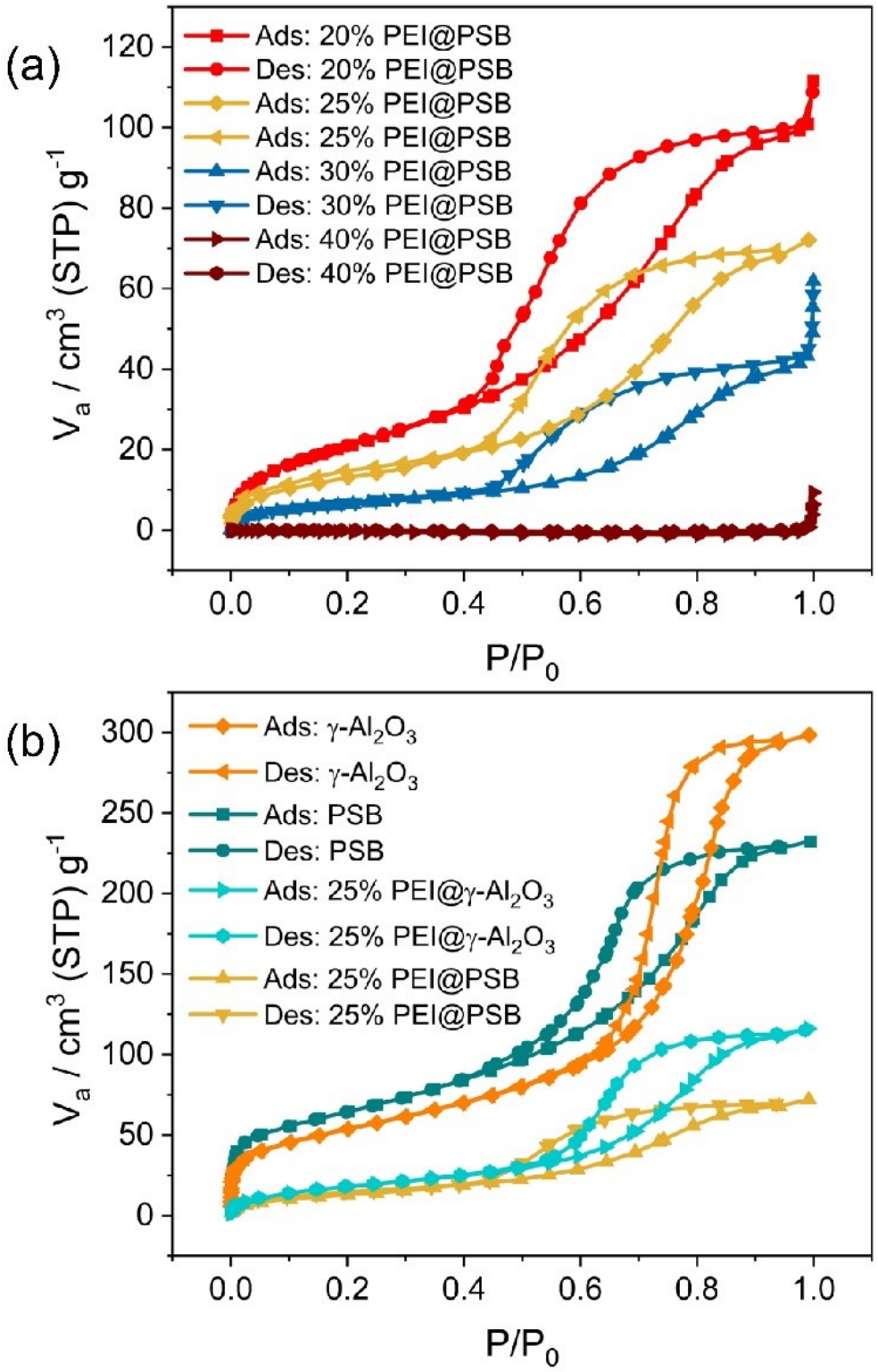

Figure S10. (a) N_2 physisorption isotherms for different loading of PEI over pseudoboehmite, and (b) N_2 physisorption isotherm comparison for as synthesized γ-Al_2O_3 from pseudoboehmite.

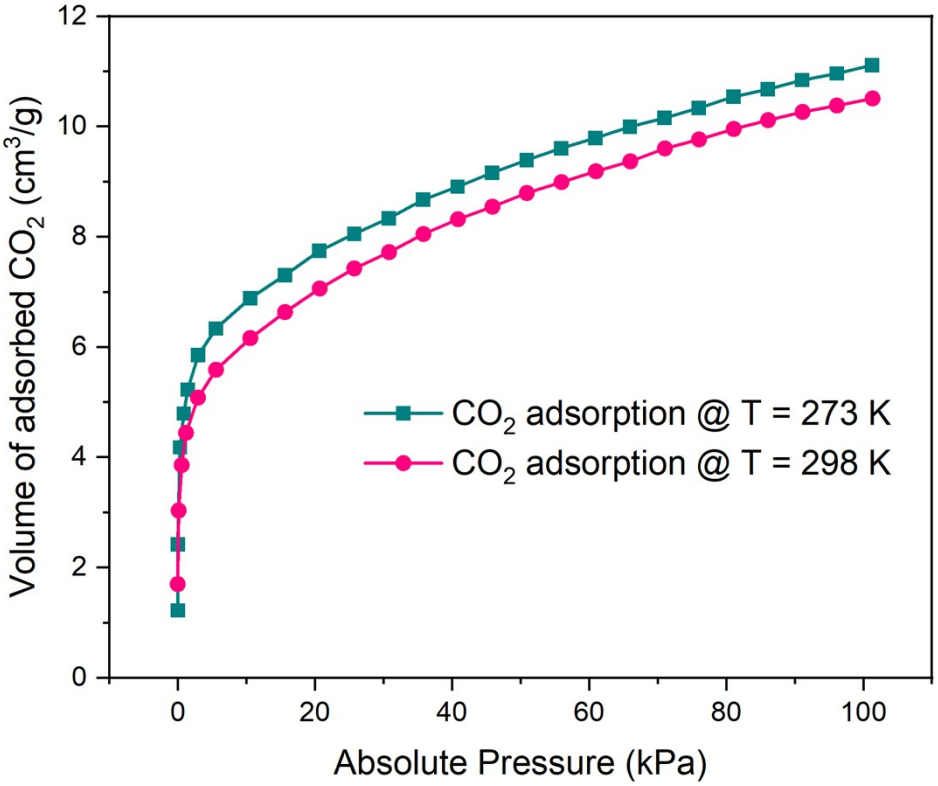

Figure S11. CO_2 adsorption isotherms for 25% PEI@PSB at two different temperatures; 273 K (0 °C) and 298 K (25 °C).

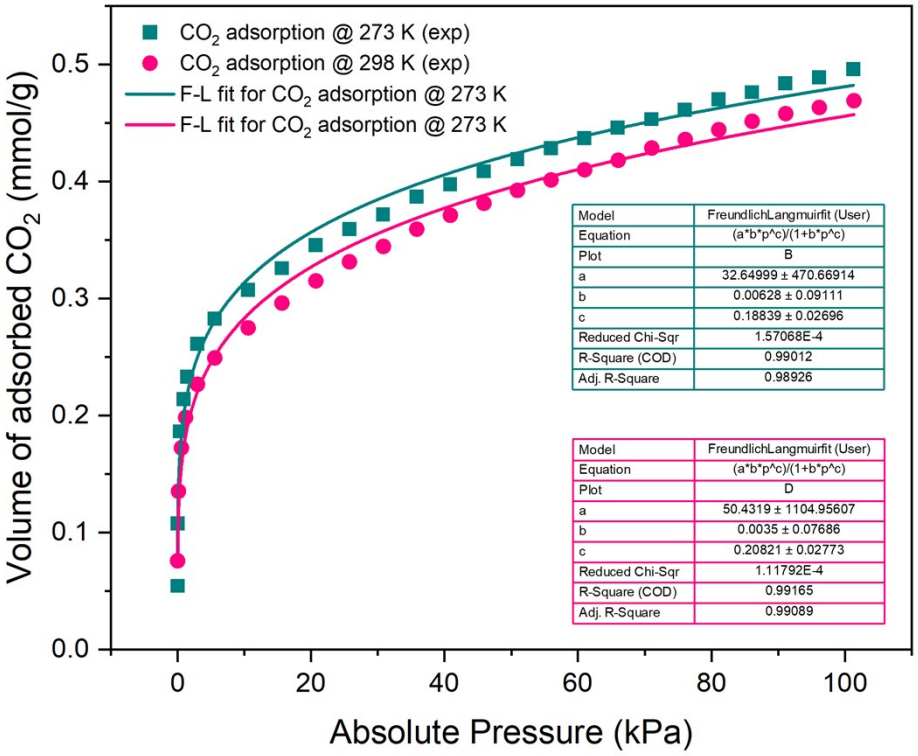

Figure S12. CO_2 adsorption isotherms for 25% PEI@PSB at two different temperatures, fitted with Freundlich-Langmuir equation (inset: parameters for non-linear curve fitting).

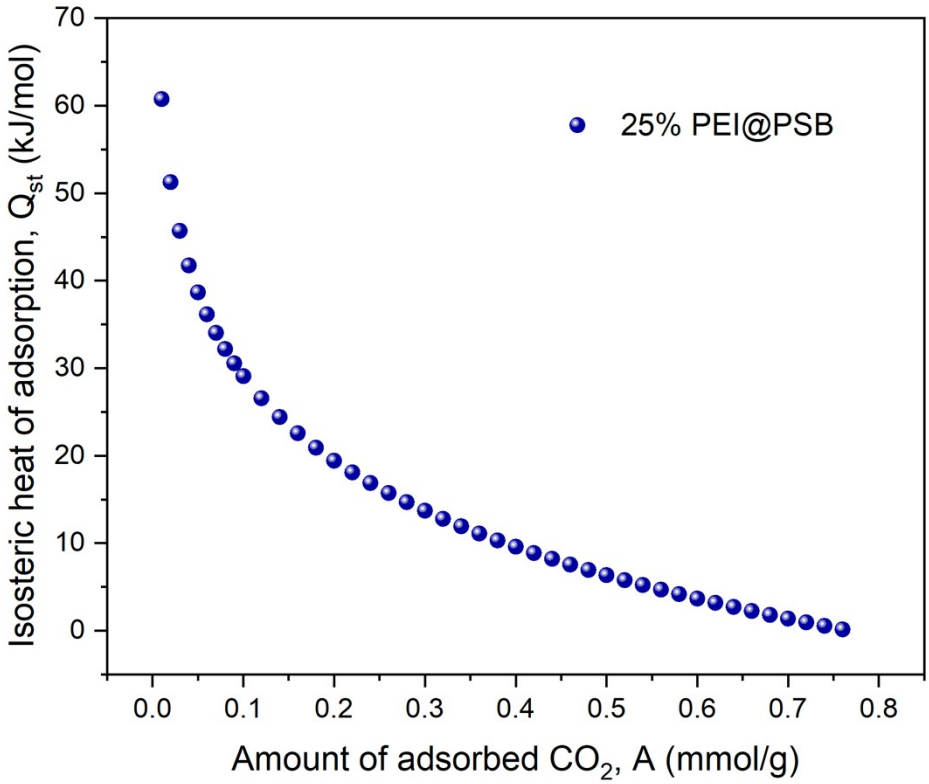

Figure S13. Isosteric heat of CO_2 adsorption over 25% PEI@PSB adsorbent based on Freundlich-Langmuir fitting.

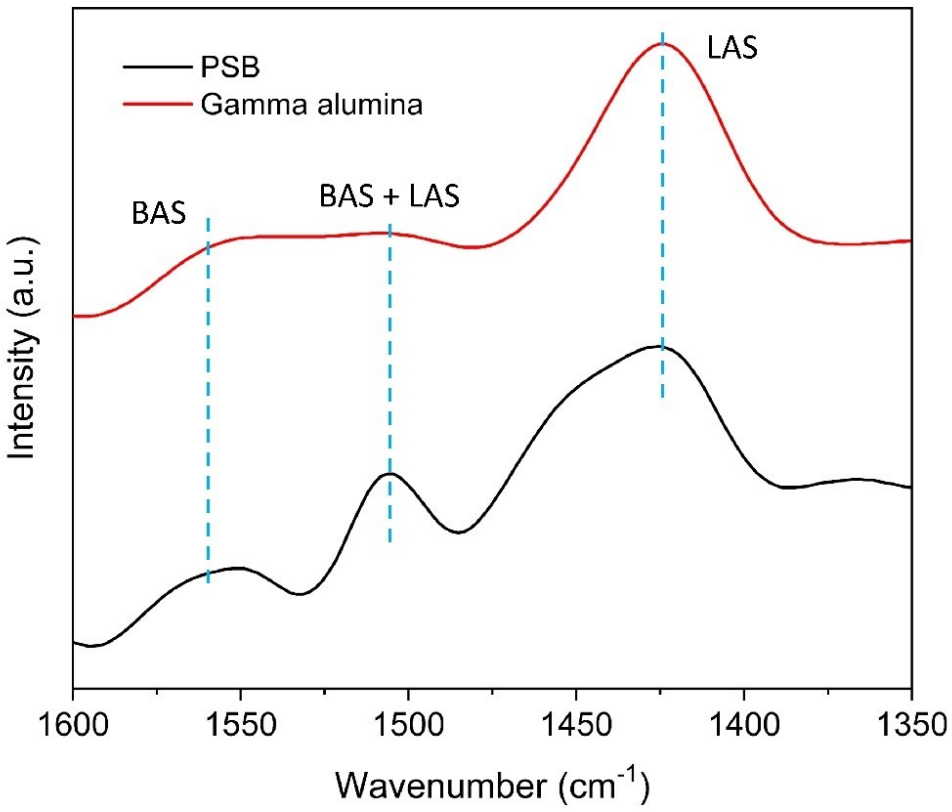

Figure S14. Pyridine-IR comparison of PSB and gamma alumina.

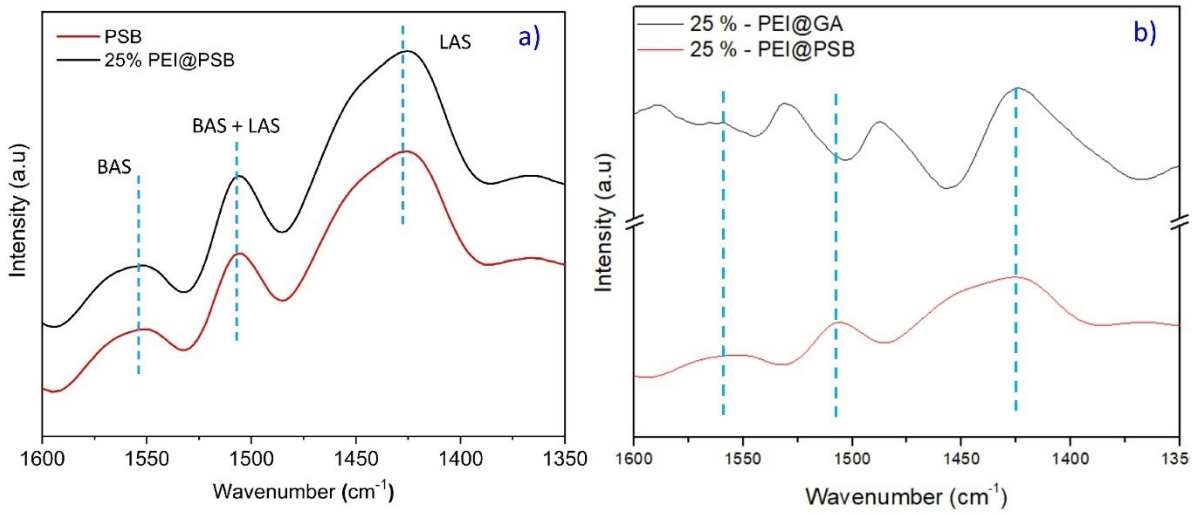

Figure S15. a) Comparison of PSB and 25% PEI@PSB, b) Comparison of 25% PEI@PSB and 25% PEI@GA

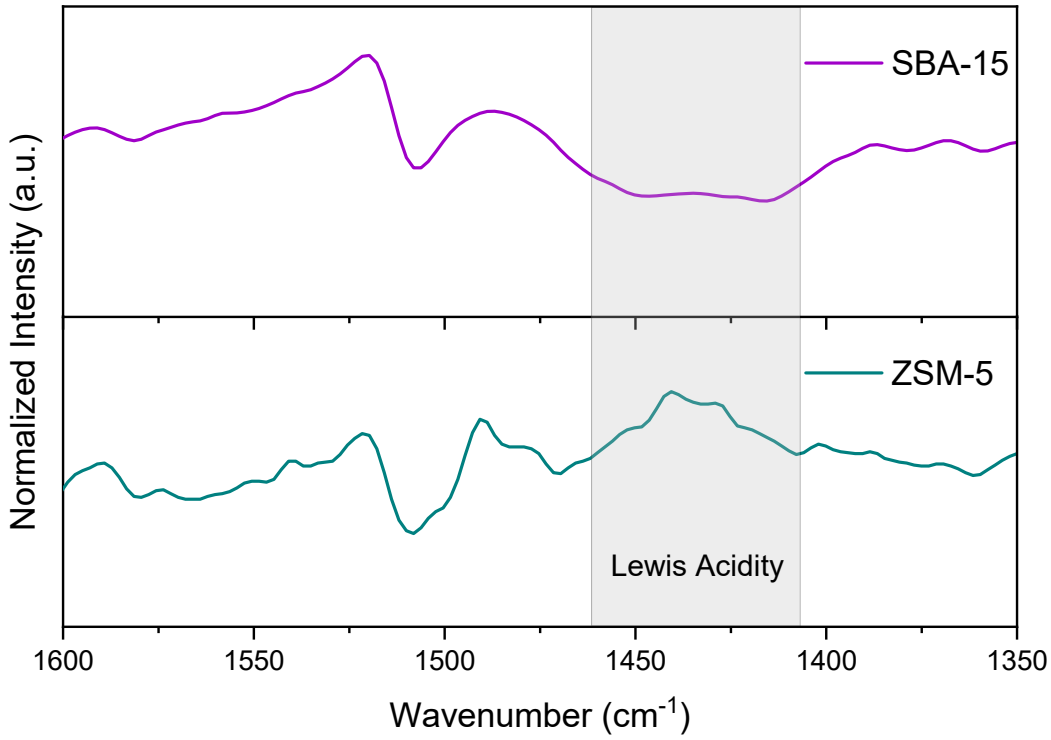

Figure S16. Pyridine IR comparison of SBA-15 and ZSM-5.

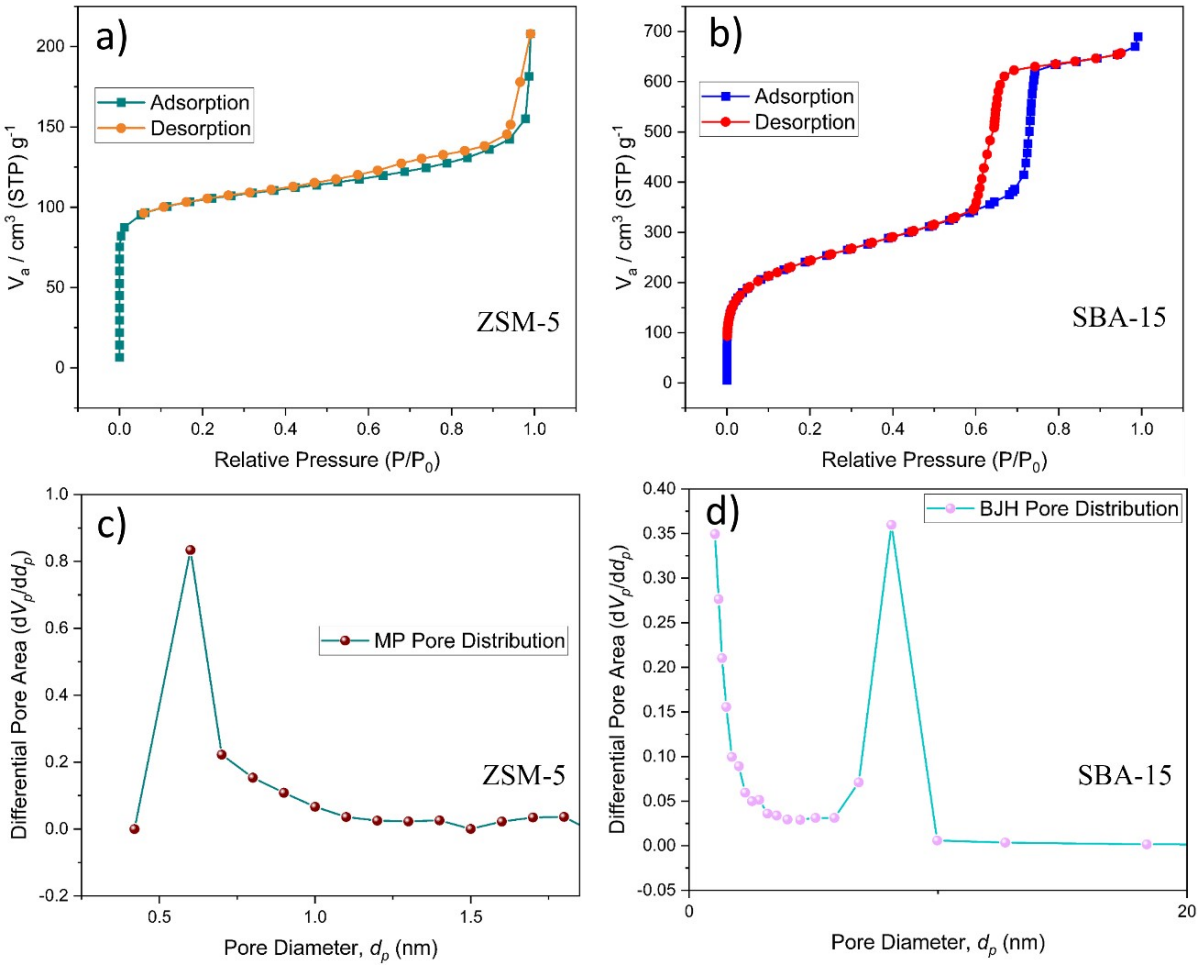

Figure S17. a) and b) Nitrogen adsorption desorption isotherms of ZSM-5 and SBA-15, c) and d) pore size distributions of ZSM-5 and SBA-15

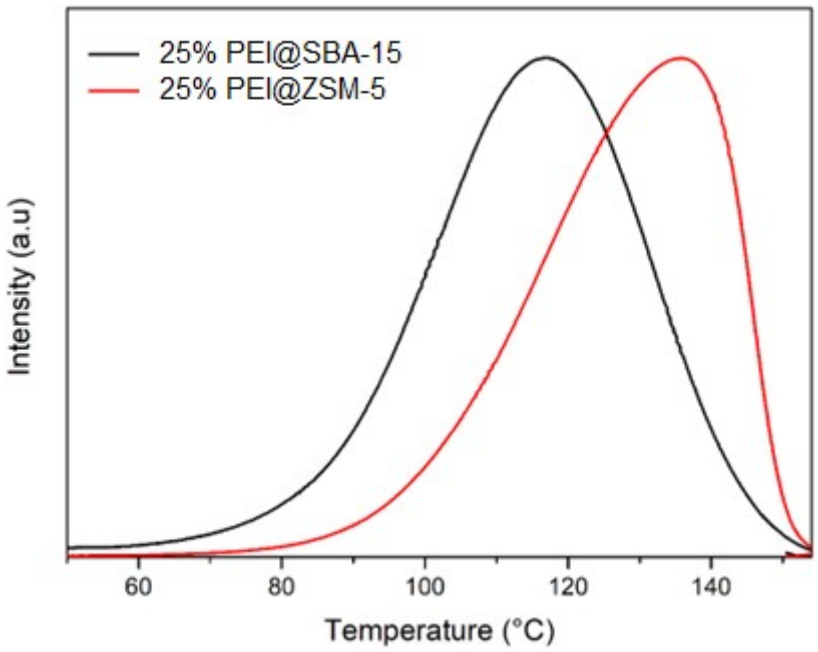

Figure S18. Comparison of CO_2-TPD profile of 25% PEI@SBA-15 with 25% PEI@ZSM-5

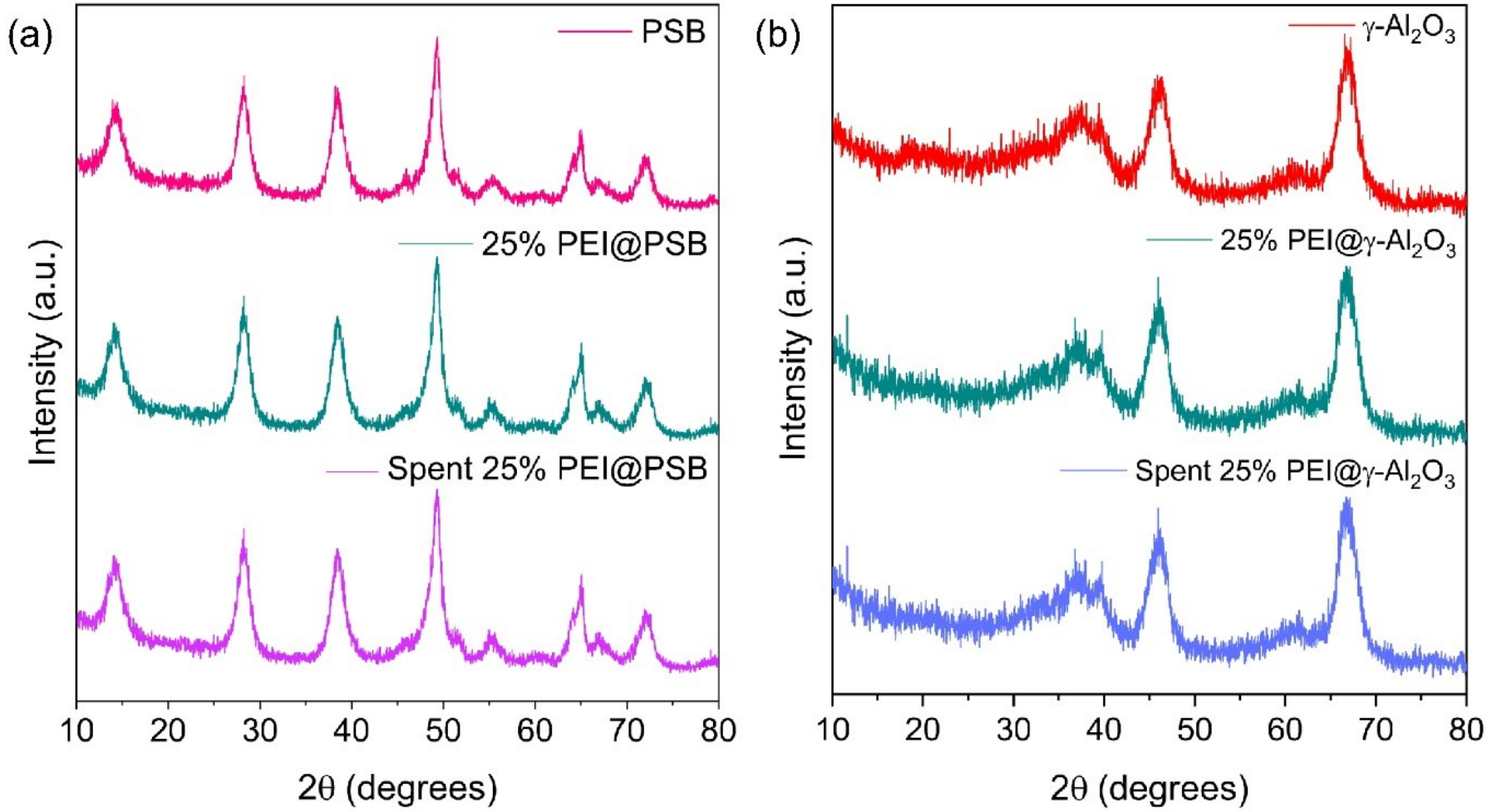

Figure S19. Comparison of XRD pattern of PEI@PSB and PEI@Al_2O_3 with unmodified and spent materials.

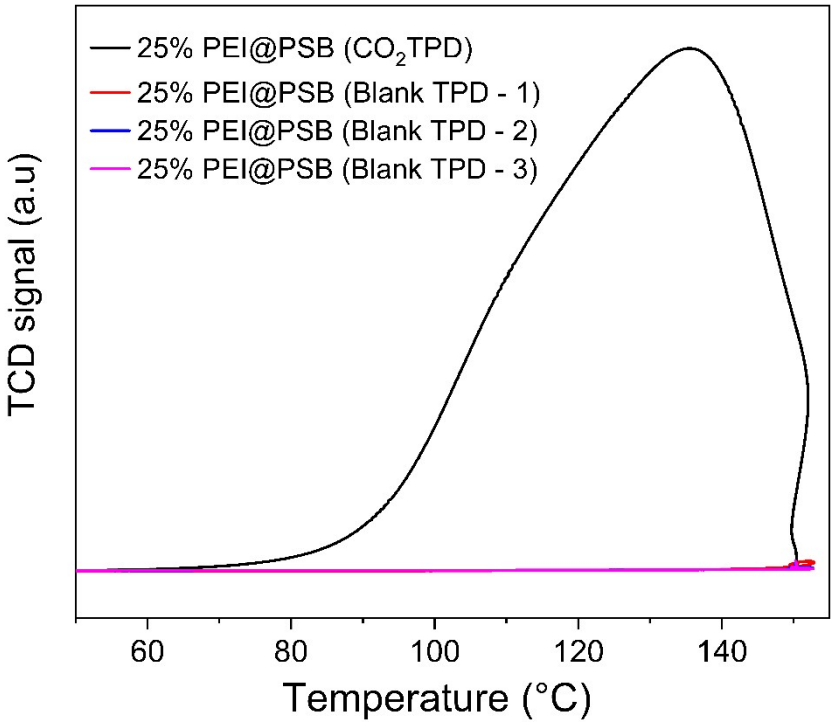

Figure S20. Comparison of blank TPD with CO_2 TPD of 25% PEI@PSB.

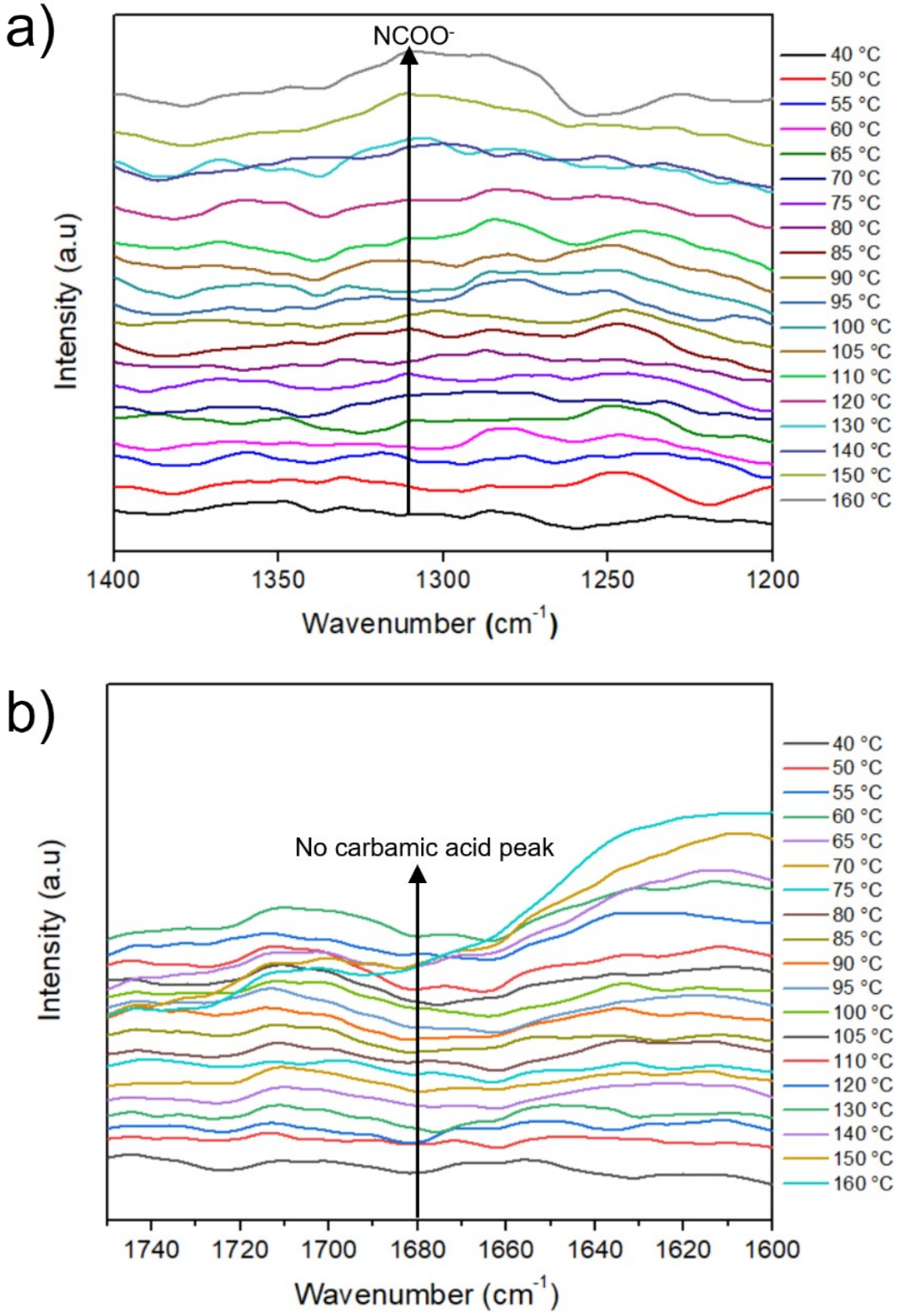

Figure S21. a) and b) temperature dependant in-situ IR analysis of 25% PEI@PSB.

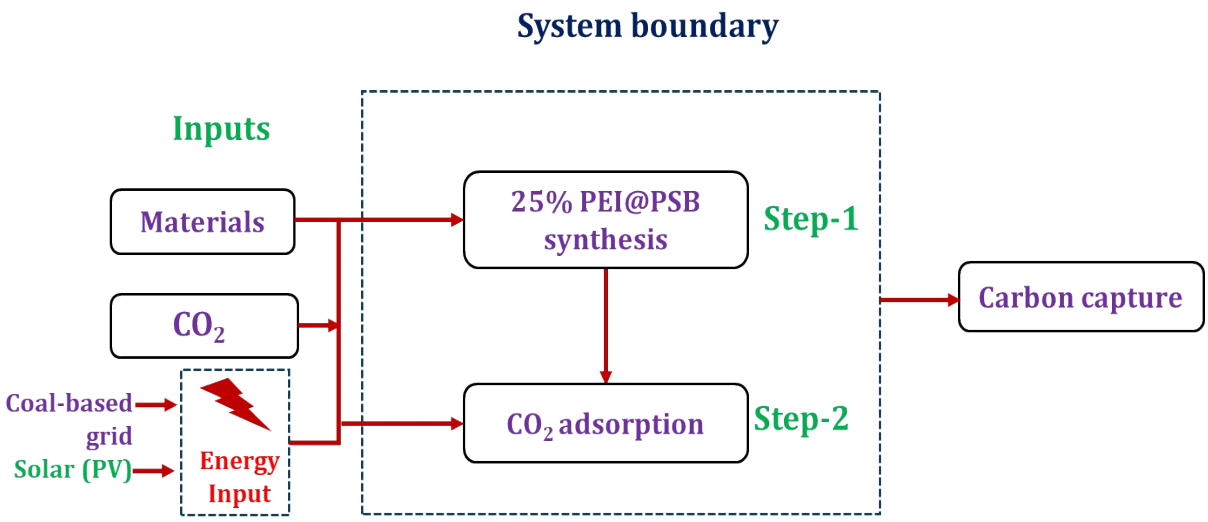

Figure S22. System boundary for PEI@PSB adsorbent synthesis, and 1 ton carbon capture.

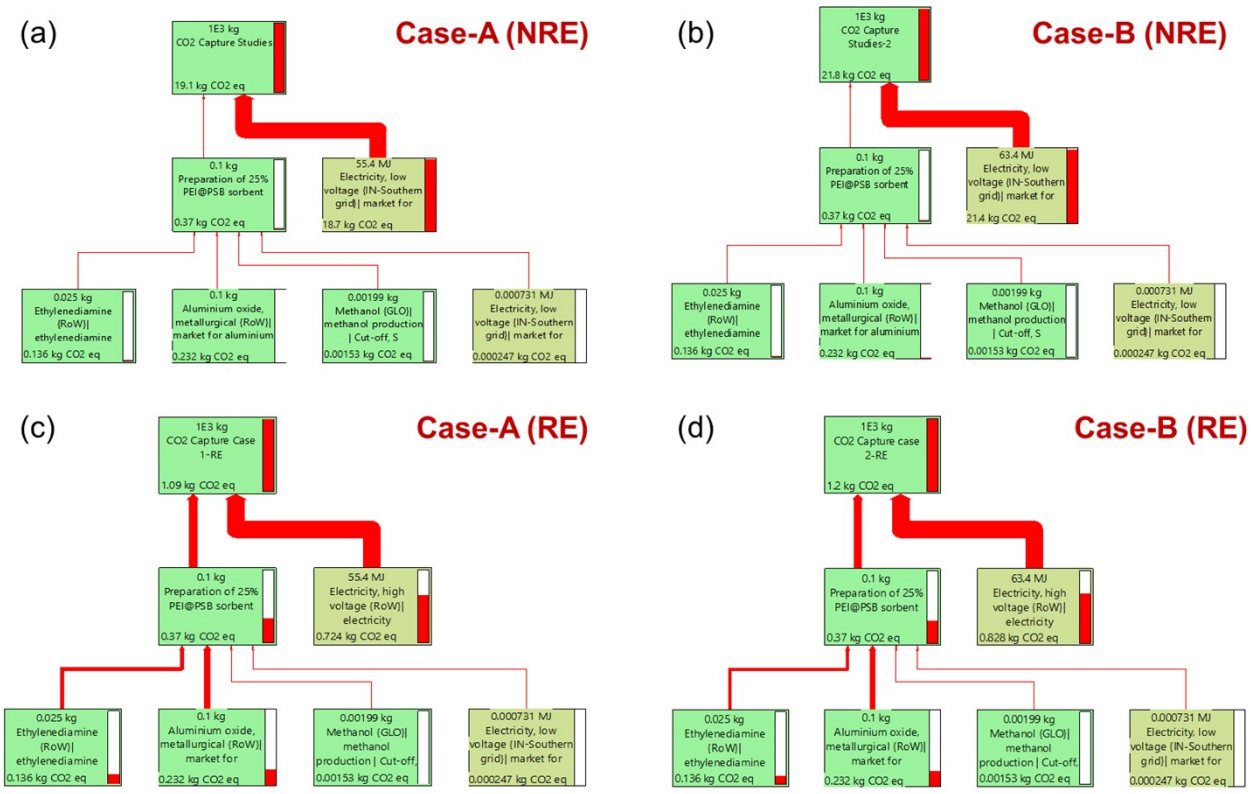

Figure S23. Sankey representation of carbon dioxide emissions for 1 ton carbon capture: (a) Case-A in NRE condition; (b) Case-B in NRE condition; (c) Case-A in RE condition; and (d) Case-B in RE condition.

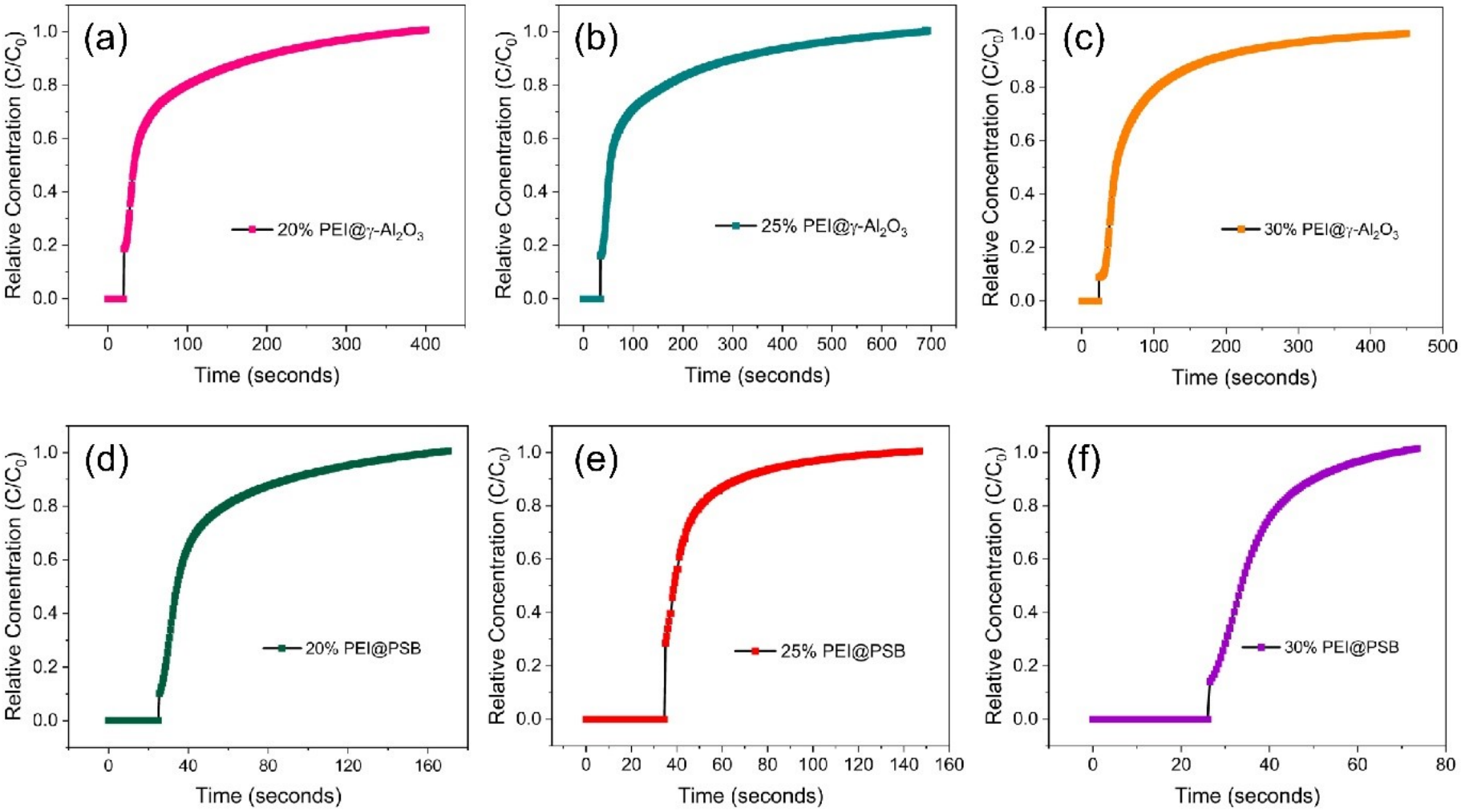

Figure S24. Dynamic breakthrough curve for CO_2 uptake experiment performed with 5000 ppm CO_2 in air. (a) 20% PEI γ-Al_2O_3 (b) 25% PEI γ-Al_2O_3 (c) 30% PEI γ-Al_2O_3 (d) 20% PEI@PSB (e) 25% PEI@PSB and (f) 30% PEI@PSB.

References

1. E. A. R. Zuiderveen, C. Caldeira, T. Vries, N. J. Schenk, M. A. J. Huijbregts, S. Sala, S. V. Hanssen and R. van Zelm, *ACS Sustainable Chem. Eng.*, 2024, **12**, 5092-5104.
2. C. Prakash, S. Singh, H. Kopperi, S. Ramakrihna and S. V. Mohan, *J. Cleaner Prod.*, 2021, **289**, 125164.
3. H. Kopperi and S. V. Mohan, *Front. Bioeng. Biotechnol.*, 2022, **10**.
4. J. Koornneef, T. van Keulen, A. Faaij and W. Turkenburg, *Int. J. Greenhouse Gas Control*, 2008, **2**, 448-467.
5. F. Li, F. Chang, J. Lundgren, X. Zhang, Y. Liu, K. Engvall and X. Ji, *ACS Sustainable Chem. Eng.*, 2023, **11**, 2810-2818.
6. K. de Kleijne, M. A. J. Huijbregts, F. Knobloch, R. van Zelm, J. P. Hilbers, H. de Coninck and S. V. Hanssen, *Nat. Energy*, 2024, DOI: 10.1038/s41560-024-01563-1.
7. M. A. J. Huijbregts, Z. J. N. Steinmann, P. M. F. Elshout, G. Stam, F. Verones, M. Vieira, M. Zijp, A. Hollander and R. van Zelm, *Int. J. Life Cycle Assess.*, 2017, **22**, 138-147.
8. X. Zhang, M. Schwarze, R. Schomäcker, R. van de Krol and F. F. Abdi, *Nat. Commun.*, 2023, **14**, 991.
9. Á. Galán-Martín, V. Tulus, I. Díaz, C. Pozo, J. Pérez-Ramírez and G. Guillén-Gosálbez, *One Earth*, 2021, **4**, 565-583.
10. J. Huo, Z. Wang, C. Oberschelp, G. Guillén-Gosálbez and S. Hellweg, *Green Chem.*, 2023, **25**, 415-430.
11. A. Sternberg, C. M. Jens and A. Bardow, *Green Chem.*, 2017, **19**, 2244-2259.
12. V. Zeleňák, M. Badaničová, D. Halamová, J. Čejka, A. Zukal, N. Murafa and G. Goerigk, *Chem. Eng. J.*, 2008, **144**, 336-342.
13. X. Xu, C. Song, J. M. Andresen, B. G. Miller and A. W. Scaroni, *Energy Fuels*, 2002, **16**, 1463-1469.
14. A. Cherevotan, J. Raj and S. C. Peter, *J. Mater. Chem. A*, 2021, **9**, 27271-27303
15. A. Heydari-Gorji, Y. Belmabkhout and A. Sayari, *Langmuir*, 2011, **27**, 12411-12416.
16. X. Xu, C. Song, J. M. Andresen, B. G. Miller and A. W. Scaroni, *Microporous Mesoporous Mater.*, 2003, **62**, 29-45.
17. X. Ma, X. Wang and C. J. J. o. t. A. C. S. Song, *J. Am. Chem. Soc.*, 2009, **131**, 5777-5783.
18. S. Jeon, H. Jung, S. H. Kim and K. B. Lee, *ACS Appl. Mater. Interfaces*, 2018, **10**, 21213-21223.
19. X. Liu, X. Qiu, X. Sun, L. Mei, L. Wang and Q. Guo, *Environ. Prog. Sustainable Energy*, 2021, **40**, e13476.
20. G. Qi, L. Fu, B. H. Choi and E. P. Giannelis, *Energy Environ. Sci.*, 2012, **5**, 7368-7375.
21. C. Li, F. Yan, X. Shen, F. Qu, Y. Wang and Z. Zhang, *Chem. Eng. J.*, 2021, **409**, 128117.
22. X. Yan, Y. Zhang, K. Qiao, X. Li, Z. Zhang, Z. Yan and S. Komarneni, *J. Hazard. Mater.*, 2011, **192**, 1505-1508.
23. X. Shen, F. Yan, C. Li, F. Qu, Y. Wang and Z. Zhang, *Environ. Sci. Technol.*, 2021, **55**, 5236-5247.
24. C. Chen and W.-S. Ahn, *Chem. Eng. J.*, 2011, **166**, 646-651.
25. M. E. Potter, K. M. Cho, J. J. Lee and C. W. Jones, *ChemSusChem*, 2017, **10**, 2192-2201.
26. K. Bhowmik, A. Chakravarty, S. Bysakh and G. De, *Energy Technol.*, 2016, **4**, 1409-1419.
27. M. Auta and B. Hameed, *Chem. Eng. J.*, 2014, **237**, 352-361.
28. N. J. Vickers, *Curr. Biol.*, 2017, **27**, R713-R715.

29. K. Li, J. Jiang, S. Tian, F. Yan and X. Chen, *J. Mater. Chem. A*, 2015, **3**, 2166-2175.
30. Y. Meng, J. Jiang, Y. Gao, F. Yan, N. Liu and A. Aihemaiti, *J. CO_2 Util.*, 2018, **27**, 89-98.
31. F. Yin, L. Zhuang, X. Luo and S. Chen, *Appl. Surf. Sci.*, 2018, **434**, 514-521.
32. W. Choi, K. Min, C. Kim, Y. S. Ko, J. W. Jeon, H. Seo, Y.-K. Park and M. Choi, *Nat. Commun.*, 2016, **7**, 1-8.